

A SPECTRAL SOLENOIDAL-GALERKIN METHOD FOR THERMAL CONVECTION UNDER THE INFLUENCE OF ROTATION AND OBLIQUE MAGNETIC FIELD

D. YARIMPABUC¹, H.I. TARMAN² and C. YILDIRIM³

¹Department of Mathematics, Osmaniye Korkut Ata University, Osmaniye, TURKEY,

²Department of Engineering Science, Middle East Technical University, Ankara, TURKEY,

³Department of Mechanical Engineering, Akdeniz University, Antalya, TURKEY.

E-mail address of corresponding author: durmusyarimpabuc@osmaniye.edu.tr

Abstract: The effects of a uniform rotation in the vertical direction and a uniform oblique magnetic field on thermal convection between rigid plates are simulated numerically. Solenoidal-Galerkin method is based on solenoidal basis functions that satisfy the boundary conditions and divergence-free conditions for both the velocity and the inclined magnetic field, exactly. The bases for thermal field are also constructed to satisfy the boundary conditions. The governing partial differential equations are reduced to a system of ordinary differential equations under Galerkin projection and subsequently integrated in time, numerically.

1 Introduction

In many astrophysical and geophysical phenomena, hydromagnetic convection in a rotating fluid layer plays an important role. In particular, the effects of rotation and magnetic field along a vertical axis on thermal convection in a horizontal fluid layer is one of the most studied problem in the convective flows due to its ease in studying the onset of instability and geometric simplicity.

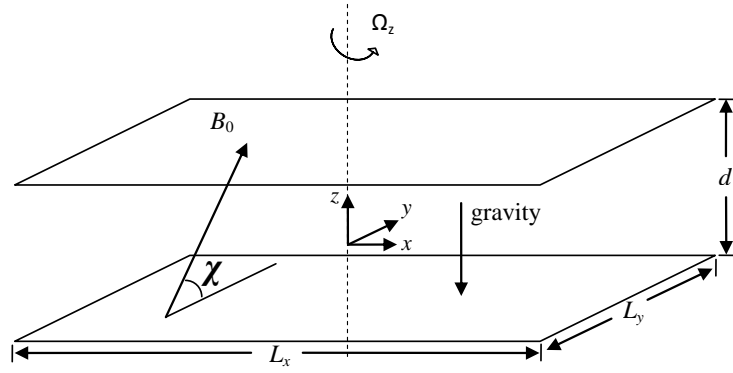
The onset of thermal instability in the Bénard layers under the effects of uniform magnetic field and rotation was first studied by Chandrasekhar [1]. It was shown that the magnetic field and rotation together delayed the onset of convection. Nakagawa performed some experimental studies on the action of magnetic field and rotation to understand the instability in a layer when the numerical and theoretical approaches are limited [3]. Although both rotation and magnetic field have inhibition effects on onset of convection, it is also found that acting together both rotation and magnetic field oppose each other such that critical Rayleigh number for the onset of convection for rotation or magnetic field acting separately is larger than that when both present, [2, 4, 5].

In this work, solenoidal bases are used to expand the velocity field in a Galerkin projection onto dual solenoidal bases so that the pressure which comes without boundary condition is eliminated. Solenoidal bases for the magnetic field are generated from the solenoidal bases for velocity by utilizing a quasi-steady relationship between the velocity and the induced magnetic field. All these processes reduce the burden on the numerical technique and increases the accuracy with which the divergence-free conditions are satisfied. The technique is validated in the linear case for rotating hydromagnetic convection by reproducing the marginal stability curves for varying Chandrasekhar and Coriolis numbers. Some numerical simulations are performed in the nonlinear regime and satisfactorily

compared with the literature.

2 Governing Equations

Thermal convective motion of a perfectly conducting fluid under Boussinesq approximations is considered in a periodic horizontal layer of thickness d between conducting plates that are heated from below and cooled from above under the influence of rotation about the vertical axis and a uniform magnetic field B_0 , which is applied externally in the yz plane with angle χ from y axis (Figure 1).



RotMagdoma

Figure 1: The geometry of the periodic convective domain

The nondimensionalization is performed in accordance with [2] except for the length scale which is based on the half depth $d_h = \frac{1}{2}d$ for computational convenience. Therefore, the dimensionless form of the governing equations are:

$$\nabla \cdot \mathbf{u} = 0, \quad (1)$$

$$\frac{\partial \mathbf{u}}{\partial t} = -(\mathbf{u} \cdot \nabla) \mathbf{u} - \nabla \Pi + Pr Ra_h \Theta \mathbf{e}_z + Pr \nabla^2 \mathbf{u} + Q_h Pr (\mathbf{e}_B \cdot \nabla) \mathbf{b} - 2Pr \Omega_h \mathbf{e}_z \times \mathbf{u}, \quad (2)$$

$$\frac{\partial \Theta}{\partial t} + (\mathbf{u} \cdot \nabla) \Theta = \frac{u \cdot \mathbf{e}_z}{2} + \nabla^2 \Theta, \quad (3)$$

$$\nabla^2 \mathbf{b} = -(\mathbf{e}_B \cdot \nabla) \mathbf{u}, \quad (4)$$

$$\nabla \cdot \mathbf{b} = 0, \quad (5)$$

with

$$\mathbf{e}_B = \text{Cos} \chi \mathbf{e}_y + \text{Sin} \chi \mathbf{e}_z \quad (6)$$

where Π denotes the pressure, $\mathbf{u} = (u, v, w)$ the velocity vector, $\mathbf{b} = (b_x, b_y, b_z)$ the induced magnetic field and Θ is the deviation from the linear conductive temperature profile. Here,

\mathbf{e}_y and \mathbf{e}_z are unit vectors in horizontal y -direction and vertical z -direction, respectively. The resulting dimensionless numbers are:

$$Ra = \frac{g\alpha \Delta T d^3}{\kappa\nu}, \quad Q = \frac{B_0^2 d^2}{\rho\mu\nu\lambda}, \quad \Omega = \frac{\Omega_z d^2}{\nu}, \quad Pr = \frac{\nu}{\kappa}, \quad (7)$$

Rayleigh ($Ra = 8Ra_h$), Chandrasekhar ($Q = 4Q_h$), the Coriolis parameter ($\Omega = 4\Omega_h$) and Prandtl (Pr), respectively. The appearance of Ra_h , Q_h and Ω_h in equation (2) is due to the use of half-depth as the length scale. Here, g denotes acceleration of gravity, α the thermal expansion coefficient, κ the thermal diffusivity, ν the kinematic viscosity, ρ the density, μ the magnetic permeability, λ the magnetic diffusivity and Ω_z the rotation rate about the vertical axis. Magnetic field in the dimensionless form becomes

$$\mathbf{B} = \text{Cos}\chi\mathbf{e}_y + \text{Sin}\chi\mathbf{e}_z + \frac{\kappa}{\lambda}\mathbf{b} \quad (8)$$

which indicates that the induced magnetic field \mathbf{b} is weak compared to the externally imposed uniform magnetic field B_0 under the limit $\kappa \ll \lambda$. Thus \mathbf{b} can be viewed as a slaved variable prescribed by the velocity field as stated by the quasi-steady relationship (4). Liquid metals or melts are characterized by this limit.

We assume that the flow takes place in a doubly periodic three-dimensional rectangular region Ω in Fig. 1 with aspect ratio $s_x \times s_y \times 2$ or $\Gamma [\frac{1}{2}s_x : \frac{1}{2}s_y]$ such that

$$0 \leq x \leq s_x, \quad 0 \leq y \leq s_y, \quad -1 \leq z \leq 1, \quad (9)$$

where $s_x = L_x/d_h$ and $s_y = L_y/d_h$ are the dimensionless periods in the horizontal x and y directions, respectively. While periodic boundary conditions are used for all the dependent variables in the horizontal directions, the boundary conditions at the perfectly conducting plates in the vertical that are maintained at constant temperatures take the form

$$\mathbf{u} = 0 \quad \text{and} \quad \frac{\partial b_x}{\partial z} = \frac{\partial b_y}{\partial z} = b_z = \Theta = 0 \quad \text{at} \quad z = \pm 1. \quad (10)$$

3 Solenoidal Basis

Solenoidal (divergence-free) basis functions $\mathbf{V}_p(\mathbf{x})$

$$\nabla \cdot \mathbf{V}_p = 0, \quad \mathbf{V}_p(\mathbf{x})|_{z=\pm 1} = \mathbf{0}. \quad (11)$$

and for the subsequent Galerkin projection procedure, dual bases $\overline{\mathbf{V}}_p^{(j)}(\mathbf{x})$

$$\nabla \cdot \overline{\mathbf{V}}_p^{(j)} = 0, \quad \overline{\mathbf{V}}_p^{(j)} \cdot \mathbf{e}_z|_{z=\pm 1} = 0. \quad (12)$$

are constructed so that both divergence-free criteria are exactly satisfied and the pressure variable is completely eliminated in the projection. Thus, the number of equations and the number of flow variables are reduced.

The quasi-steady relationship (4) between the velocity and the magnetic field variables is used to generate the corresponding magnetic solenoidal basis functions, [7]. This is a crucial step in this approach. In order to facilitate the numerical evaluation of the Galerkin projection integrals, the solenoidal basis functions are based on the Legendre polynomials in the vertical z -direction which are so constructed to satisfy the boundary conditions.

4 Numerical Procedure:

The flow is assumed periodic in the horizontal directions that allows the use of Fourier series expansions of the dependent flow variables,

$$\begin{bmatrix} \mathbf{u} \\ \Theta \\ \mathbf{b} \end{bmatrix} (x, y, z, t) = \sum_{m,n} \begin{bmatrix} \hat{\mathbf{u}} \\ \hat{\Theta} \\ \hat{\mathbf{b}} \end{bmatrix} (m, n, z, t) e^{(i\xi_m x + i\eta_n y)} \quad (13)$$

where $\xi_m = \frac{2\pi m}{s_x}$ and $\eta_n = \frac{2\pi n}{s_y}$ are the wave numbers with the ranges $1 - \frac{1}{2}N_x \leq m \leq \frac{1}{2}N_x$ and $1 - \frac{1}{2}N_y \leq n \leq \frac{1}{2}N_y$ for the indices m and n . The vertical profiles for velocity and the magnetic fields are further expanded in terms of the solenoidal bases

$$\hat{\mathbf{u}}(m, n, z, t) = \sum_{p=0}^M a_p^{(1)}(t) \mathbf{V}_p^{(1)}(z) + a_p^{(2)}(t) \mathbf{V}_p^{(2)}(z), \quad (14)$$

$$\hat{\mathbf{b}}(m, n, z, t) = \sum_{p=0}^M a_p^{(1)}(t) \mathbf{B}_p^{(1)}(z) + a_p^{(2)}(t) \mathbf{B}_p^{(2)}(z). \quad (15)$$

The velocity and magnetic fields share the same time evolution as dictated by the quasi-steady link stated in (4). The expansion for the thermal field is

$$\hat{\Theta}(m, n, z, t) = \sum_{p=0}^M b_p(t) T_p(z), \quad (16)$$

where $T_p(z) = (1 - z^2)L_p(z)$ with its dual $\bar{T}_p(z) = L_p(z)$. The evolution of the time dependent expansion coefficients $a_p^{(j)}(t)$ and $b_p(t)$ is determined by numerically integrating the projected equations in time. For the numerical evaluation of the inner product integrals arising in the projection procedure, Gauss-Legendre-Lobatto (GLL) quadrature is used.

5 Linear Stability

Numerical experiments are performed first to determine the linear stability of the conductive (no-motion) state leading to the critical values when the convective motion just sets in for testing the solenoidal bases and the projection procedure. For this purpose, The linearized governing equations

$$\frac{\partial \mathbf{u}}{\partial t} = -\nabla \Pi + Pr Ra_h \Theta \mathbf{e}_z + Pr \nabla^2 \mathbf{u} + Q_h Pr (\mathbf{e}_z \cdot \nabla) \mathbf{b} - 2Pr \Omega_h \mathbf{e}_z \times \mathbf{u}, \quad (17)$$

$$\frac{\partial \Theta}{\partial t} = \frac{1}{2} \mathbf{e}_z \cdot \nabla \mathbf{u} + \nabla^2 \Theta \quad (18)$$

are projected onto the dual space after the substitution of the expansions in terms of the solenoidal bases. Then, they are transformed into the system of ordinary differential

equations

$$[M]_{(3 \times 3)} \begin{bmatrix} \dot{a}_p^{(1)} \\ \dot{a}_p^{(2)} \\ \dot{b}_p \end{bmatrix} = [S]_{(3 \times 3)} \begin{bmatrix} a_p^{(1)} \\ a_p^{(2)} \\ b_p \end{bmatrix} \quad (19)$$

where $[M]$, $[S]$ are mass and stiffness matrices, respectively [7]. The assumption of a time dependence in the form

$$[a^{(1)}; a^{(2)}; b] \propto \exp(\zeta t) \quad (20)$$

reduces the system to a generalized eigenvalue problem for the eigenvalues ζ .

Table 1: The critical Rayleigh number Ra_c at $Q = 1210$ for various Taylor Number ($Ta = 4\Omega^2$) values.

	Aurnou and Olson [5]	Present Work
Taylor number	$Ra_c(Nu)$	$Ra_c(Nu)$
0	27100	27101.6
11000	28300	28311.2
95000	29800	29810.5

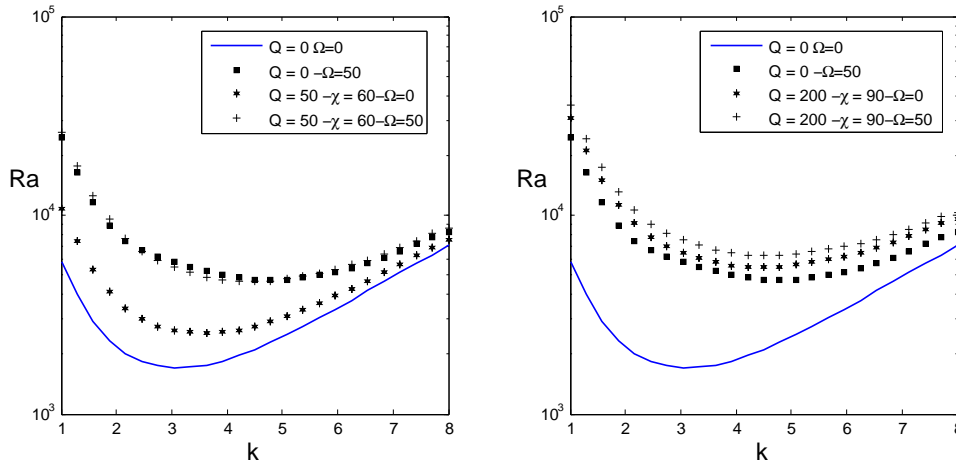


Figure 2: Marginal stability curves for different magnetic field Q and Coriolis Force Ω values.

The critical Rayleigh number Ra_c at $Q = 1210$ for various Taylor Number ($Ta = 4\Omega^2$) values, are listed in Table 1 for the rightmost eigenvalue just crossing the imaginary axis. These are obtained at the selection of $n = 1$ and $m = 0$ in (13). They are in agreement with the experimental study of Aurnou and Olson [5]. The corresponding marginal stability curves for two different cases are plotted in Figure 2. Since, only the vertical component of the magnetic field has an effect on the stability in this regime, Coriolis force dominates over the Lorentz force on the left in Figure 2, which means that the results are similar to the absence of the magnetic field. The figure on the right arises when the Lorentz force dominates over the Coriolis forces in which case the results are similar to the absence of rotation, [2, 4].

6 Nonlinear Analysis

Nonlinear governing equations are discretized in time using a semi-implicit scheme in which the non-linear advection, magnetic and rotation terms are treated explicitly using the third-order Adams Bashforth (AB3) method, and diffusion terms are discretized implicitly by third order Adams-Moulton (AM3).

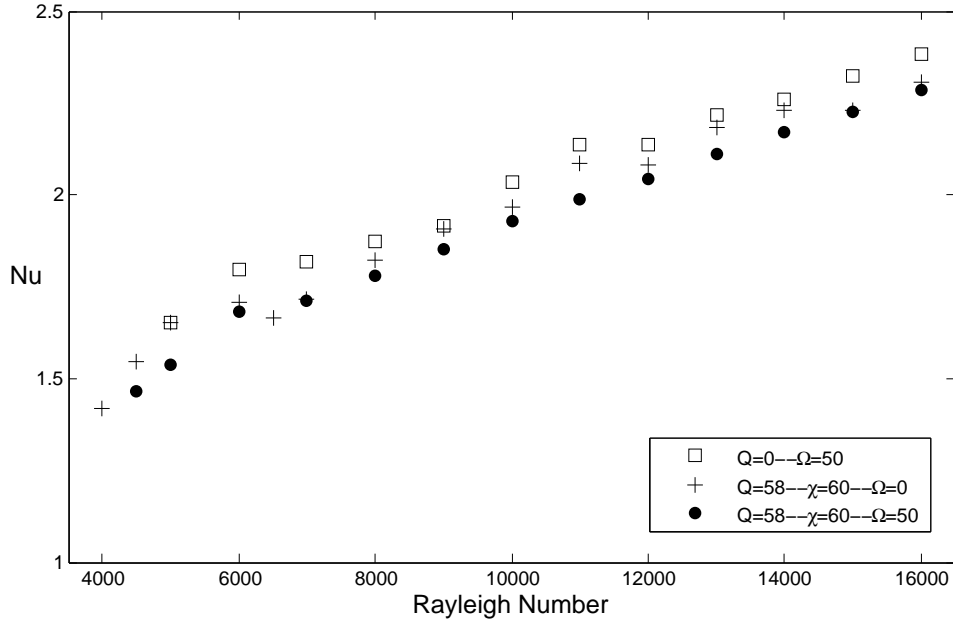


Figure 3: Nusselt versus Rayleigh number at $Pr = 0.1$, $\Gamma [3.1 : 3.0]$, $Q = 58$ with an angle $\chi = 60$ and $\Omega = 50$.

The numerical experiments are performed to study the effects of the magnetic field with an angle $\chi = 60$ and the rotation, separately and together, with varying Rayleigh number on the convective heat transport efficiency indicated by Nusselt number (Nu) which is the ratio of the heat transport with and without convection. The flow is chosen to take place in a convective box with the aspect ratio $\Gamma [3.1 : 3.0]$ for Prandtl number, $Pr = 0.1$, Chandrasekhar number $Q = 58$ with an angle $\chi = 60$ and Coriolis numbers $\Omega = 50$. Since only the vertical component of the magnetic field has an inhibition effect on the steady flow, in order to make the magnetic field and rotational effects comparable ($Q \sim Ta^{1/2}$, [5]), Chandrasekhar number $Q = 58$ is chosen. Figure 3 shows the Nusselt number versus Rayleigh number for three different cases. In the case where the Coriolis and Lorentz forces are comparable, the minimum temperature gradient for required instability is reduced when compared with the other cases where rotation and magnetic field are acting separately. This is also obtained in [2, 4, 5].

References

- [1] Subrahmanyam C.: The Instability of a Layer of Fluid Heated below and Subject to the Simultaneous Action of a Magnetic Field and Rotation. Proc. Roy. Soc. A. 225(1954) 173–184
- [2] Subrahmanyam C.: Hydrodynamics and Hydromagnetic Instability. Oxford: Clarendon Press 1961.
- [3] Y. Nakagawa.: Experiments on the instability of a layer mercury heated from below and subjected to the simultaneous action of a magnetic field and rotation. Proc. R. Soc. Lond. A. 242(1957) 81–88.
- [4] I.A. Eltayeb.: Oberstabile hydromagnetic convection in rotating fluid layer. J. Fluid Mech. 71-1(1975) 161–179.
- [5] J. M. Aurnou and P. L. Olson.: Experiments on Rayleigh Benard convection, magneto convection and rotating magneto convection in liquid gallium. J. Fluid Mech. 430(2001) 283–307.
- [6] C. Yıldırım, D. Yarımabaç and H.I. Tarman.: A Spectral Solenoidal-Galerkin Method for Rotating Thermal Convection between Rigid Plates. Mathematical Problems in Engineering. (2013) 8 pages.
- [7] D. Yarımabaç, H.I. Tarman and C. Yıldırım.: Numerical Simulations of Thermal Convection under the Influence of an Inclined Magnetic Field by Using Solenoidal Bases. .Mathematical Methods in the Applied Sciences. Accepted.